AN INVESTIGATION OF SEISMIC RESPONSE OF PRECAST CONCRETE BEAM TO COLUMN CONNECTIONS: EXPERIMENTAL STUDY

H. Shariatmadar and E. Zamani Beydokhti[*]
Department of Civil Engineering, Faculty of Engineering, Ferdowsi University of Mashhad (FUM), Postal Code 9177948944, P.O. Box 1111, Mashhad, Iran

ABSTRACT

This paper presents the test results of three precast and one monolithic connection in moment-resisting concrete frame subjected to constant axial compression and lateral reversed cyclic loads. The precast specimens had cast-in-place concrete connections with different details, namely straight spliced (PC1), U-shaped (PC2), and U-shaped with steel plate (PC3).The results for Hysteresis loops, strength, damping, energy dissipation and ductility are presented. Comparisons of performance parameters revealed that the behavior of PC1 was more similar to monolithic Specimen and it can be used in high seismic zones. The other two precast connections are recommended to be used in moderate seismic regions.

1. INTRODUCTION

Precasting has several advantages which can emulate conventional cast-in-place construction and further research is needed for more appropriate connection details. High quality control [1-3], construction efficiency, and consequently saving time and expense are some of the advantages. However, there are some problems that are resulted from assembling precast subassemblies such as beams and columns. Structurally, there are time differences between cast-in-place connection and precast subassemblies. These joints are known as the weakest links of precast load transmission and are considerably exposed to plastic hinge generation. The use of precast structures for dominantly residential purposes has increased in recent years. However, there are no special design provisions in the Iran

---

[*]E-mail address of the corresponding author: eb.zamani@stu.um.ac.ir (E. Zamani Beydokhti)

building code for precast structures and consequently all designs are performed based on cast-in-place concrete design code. For this reason, it is necessary to conduct experimental studies to evaluate the beam-column connection behavior.

A research program on the performance of ductile beam-column precast connections was developed at Ferdowsi University of Mashhad. Three precast connections including: straight spliced, U-shaped in column, and hybrid U-shaped with steel plate in beam were tested and compared with one monolithic counterpart. The specimen details were adopted with considering to constructional efficiency and ease of erection. Performance comparisons are made based on the envelope curves, stiffness degradation, energy dissipation, damping ratio and ductility factor of the different connection types. All test specimens in this research program were detailed according to the governing building codes or the available literature.

LITERATURE SURVEY

Connection detail and location between precast members is either one of the numerous experimental or analytical investigation issues for researchers. Ertas et al. [4] tested four types of cast-in-place precast (CIP) beam-column connections under reversed cyclic loading in inelastic range. Specimens were subjected to 3.5% story drift angle in ultimate loading. The hysteresis behavior of specimens cast-in-place column, cast-in-place beam, and modified bolted were similar to those of monolithic Specimen. Pinching effect and excessive bond deterioration were not observed in the CIP connections due to the use of steel fiber in the concrete and U-shaped reinforcing bars. The research of Restrepo [5] consisted of precast concrete beams placed between columns and a CIP concrete joint core which was constructed at the beam - column intersection. The test results showed that the connection can be successfully designed and constructed to emulate cast-in-place construction. Alcocer et al. [6] tested two full-scale precast beam-to-column connections under uni- or bi-directional reversed cyclic loading. Conventional mild steel reinforcing bars or prestressing strands, rather than welding or special bolts, were used to achieve beam continuity. Connection strength in both specimens was 80 percent of what obtained from monolithic reinforced concrete construction. The connection capacity was remained nearly constant up to 3.5% drift. They reported that plastic hinges developed as expected at the column face. Khoo et al. [7] introduced a modified assembled configuration for precast concrete frames in which the connections are constructed on the beam span and kept them away from the column faces. This assembly resulted to avoid coincidence of the joint region with the plastic hinge length during seismic excitations. They utilized 90 and 180 degree hooked bars within the length of equal to an effective beam depth d from the column faces. Based on the test results, significant bond deterioration was observed in the connection regions due to the insufficient anchorage length when 90-degree hooks were used. As a weakness of these systems, constructing the connections away from column faces causes difficulties in element transportation.

Some studies have been done related to prestressed and hybrid connections. Cheok et al. [8] developed post tensioned steel bars to assemble the precast elements. They reported that prestressing played an important role in continuity and shear resistance in connection. The energy was dissipated by post yielding of steel bars, whereas prestressed strands maintained

the continuity and provided the required shear resistance to the applied loads in the absence of corbels and shear keys. Pampanin et al. [9] tested high performance seismic resisting precast concrete frame systems, based on the use of unbonded post-tensioned tendons with self-centering capabilities. The results confirmed the unique ductility and efficiency of these systems as a lateral load resisting structures which is able to undergo high inelastic displacement with limited level of damage. The damage and residual displacement was negligible when compared to traditional monolithic (cast-in situ) ductile systems. Li and Leong [10] tested two hybrid precast connection types and their monolithic counterparts. They perceived that the discontinuity in bottom reinforcement of precast beams led to lower moment capacity of the specimens. Pinching also occurred due to widening the tolerances used in bolted connection.

Essentially, some mechanisms of moment and shear transmission are more favorable due to constructional speed and behavior efficiency. Bolted connections with straight and hooked bars are more useful in precast connections. Hooked bars, if provide in a good detailing will reduce the length of splicing and will be executable in the areas without enough length for straight splicing. However, it may have some imperfection in shear resistance. Shear transmission mechanism can be improved with welded or bolted plates to connect beam and column members together. Li and Leong [10] revealed that bolted plates might lose initial connection stiffness rapidly due to tolerance of holes. Also welding has some disadvantages in precast construction and it should be performed prior to casting or away from concrete.

TEST SPECIMENS AND CONNECTION DETAILS

All full scaled specimens were selected from a five story peripheral frame with two beams in one plane that were connected to column faces. Three interior precast connections (PC1, PC2 and PC3) and one monolithic counterpart (MO) were designed and manufactured according to strength and stiffness demand calculated by Canadian concrete building code (CSA-A23.3-04) [11]. The beam and column lengths and cross section dimensions were the same for all specimens. The ends of beam and column (breaking sections) were coinciding with the mid span and mid story height, respectively; which in fact were contra flexure points of moment diagram under lateral load. Free span length and beam cross section were 200 cm (79″) and 40x40 cm (15.75″x15.75″), respectively. Total column length from bottom to top was 320 cm (126"). The precast concrete designed to achieve a cylindrical compressive strength of about 28 MPa (4 ksi) and design yield stress of the steel bars assumed to be 400 MPa (57 ksi). Material properties for the precast and cast-in-place concrete and steel reinforcing bars are presented in Table 1, Table 2 and Table 3.

Table 1: Mixture design for precast and cast-in-place concrete

Material	Coarse Agg	Fine Agg	Sand	Water	Cement
Weight (kg/m^3)	373	318	1272	165	300

W/C Ratio= 0.55

Table 2: Material properties of concrete in specimens

Compressive Cylindrical Strength (MPa)		MO	PC1	PC2	PC3
At 28 Days		28.3	28.3	28.3	28.3
At Testing	Monolithic Concrete	28.7	---	---	---
	Precast Concrete	---	28.7	28.8	28.6
	Cast-in-Place Concrete	---	25.4	25.7	25.8

Table 3: Material properties of steel rebars

Bar Size (mm)	F_y (MPa)	Mean F_y (MPa)	F_u (MPa)	Mean F_u (MPa)
16	512.4 507.4	509.9	651.7 651.7	651.7
18	529.4 537.2	533.3	690 702	696
20	533.3 494	513.65	674.5 643	658.75
22	439.2 384.3	411.75	627.4 576.4	601.9
28	407.8 423.3	415.55	545 603.9	574.45

Mixture design of cast-in-place concrete in laboratory was similar to that of precast members and monolithic Specimen (MO). In addition, non-shrinking grout was used in concrete of connections to avoid shrinkage and shrinking cracks between precast elements. Since slab reinforcements were placed and casted with precast beams in real construction, 10 cm (4") in top of precast beams remained without concrete so that it was filled with joint, simultaneously.

MONOLITHIC SPECIMEN

Monolithic Specimen (MO) was developed for comparing and evaluating results of precast specimens. It was designed according to Canadian cast-in-place (CIP) concrete recommendations (CSA-A23.3-04) [11]. As shown in Fig. 1 the column longitudinal reinforcement was 8 Φ 18 for all specimens (monolithic and precast concrete). Spacing between the closed stirrups Φ 10 was approximately 125 mm (5″) within the 70 cm (27.5″) top and bottom of beam-column joint core and 250 mm at the remaining length of column. The top and bottom longitudinal bars of beams were 2 Φ 18 and 3 Φ 16, respectively, where some ADD-bars were required to be added to this rebars. The ADD-bars placed in connection region were 2 Φ 28 and 2 Φ 22 at the top and bottom, respectively. Top ADD-bars had 320 cm (126″) and bottom ADD-bars had 240 cm (95″) length. Top ADD-bars were increased in diameter for realization due to gravity load effect.
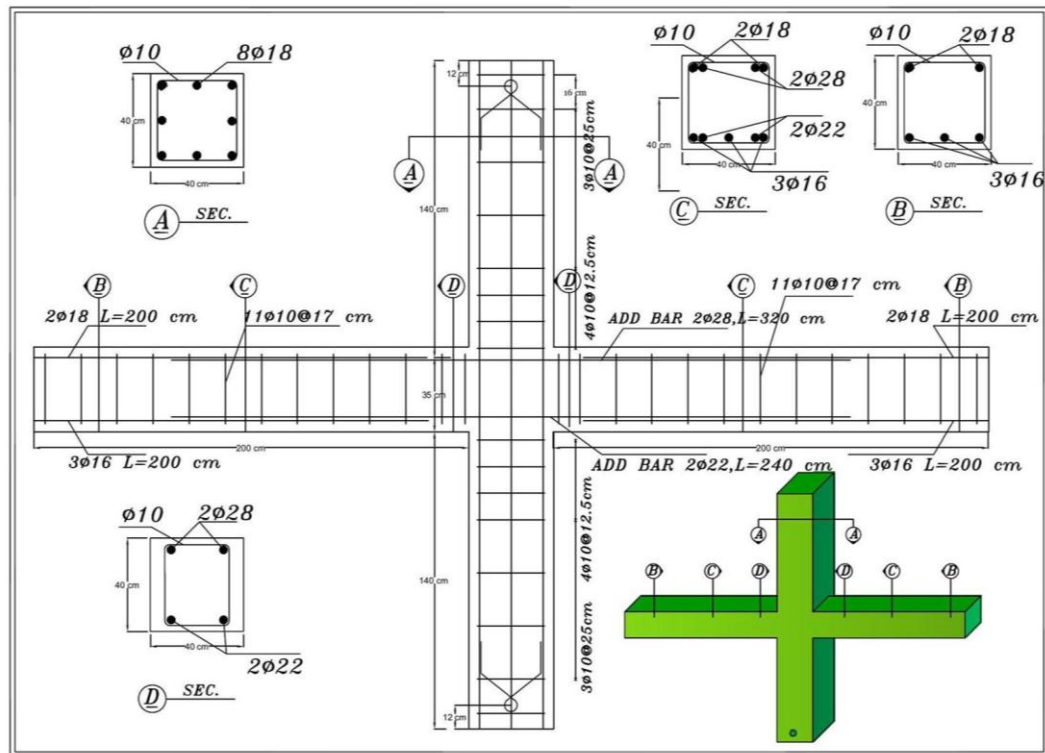
Figure 1. Dimensions and reinforcement details of Monolithic Specimen

STRAIGHT SPLICED SPECIMEN (PC1)

The design concept of straight spliced Specimen (PC1) has the most striking similarity with Specimen MO as shown in Fig. 2. This concept has been tested by Park et al. [12], Lee et al. [13] and Khaloo et al. [14, 15] which is widely used in building industry. There were no transverse bars in connection length region. Column reinforcing was the same as MO (8 Φ 18). There was a gap at mid-length of the precast concrete column where the height of this gap 350 mm (13.8″). A free box-shaped space was provided in PC1 beams at the vicinity of column face for placing the ADD-bars. The length of free space was 2100 mm (82.7″) which was about 27.5% of clear span length of beams. At the top of precast beams, 10 cm (4″) left empty in all precast specimens which had been filled with concrete during the specimen assembly for realization due to slab connection. The number and diameter of main longitudinal and ADD-bars of PC1 beams and columns were the same as those of specimen MO. After placing the beams at the axe of the column gap and entering the ADD-bars in beam and column free gap, 10 cm top of precast beams, and free spaces of column and beam were filled simultaneously with cast-in-place concrete. Tensile strength of rebars and compressive strength of precast concrete were equal to those of specimen MO.
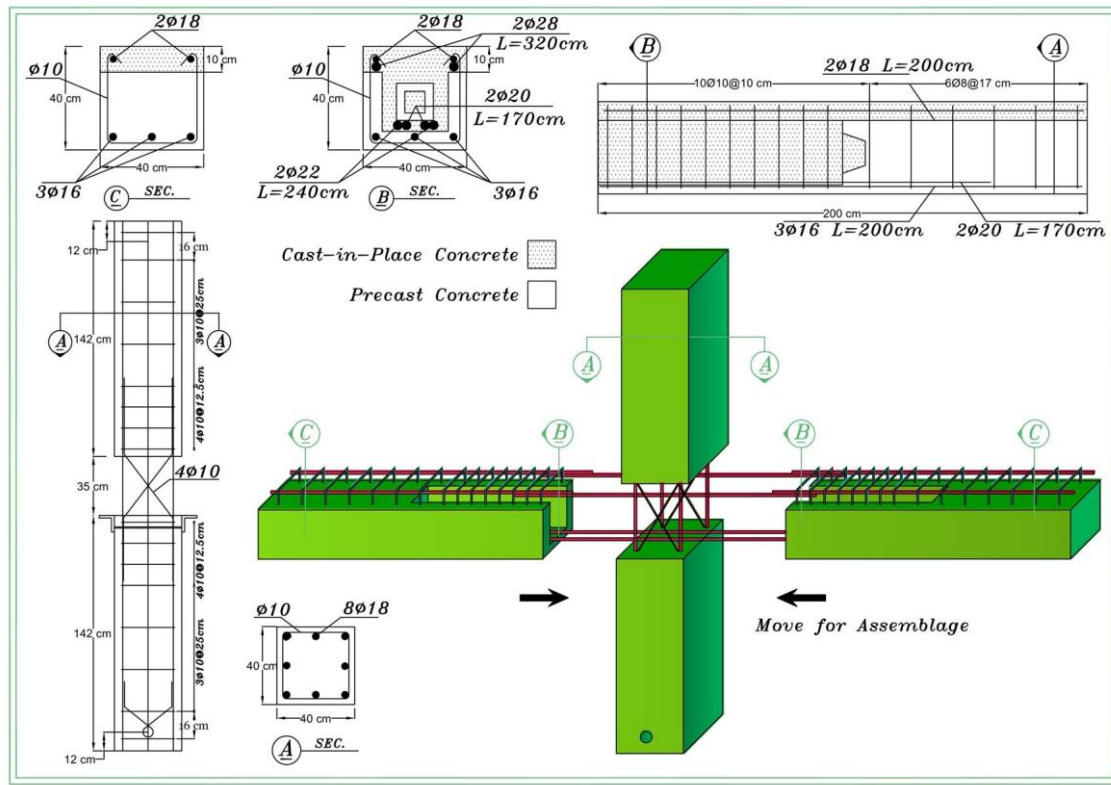
Figure 2. Dimensions and reinforcement details of Specimen PC1

U-SHAPED REBAR SPECIMEN (PC2)

Details of U-shaped Specimen (PC2) are presented in Fig. 3. The purpose of using U-shaped rebars was to minimize the splice length of field working area in vicinity of column faces. The provision of hooked bar anchorage is necessary to enable the development of full strength in rebar and to ensure the transfer of bond stress. The column configuration and details of U-shaped Specimen PC2 was exactly similar to the column of specimen PC1. Two U-shaped rebars in beams were entered into the free gap of column at mid-height from each side. Four U-shaped rebars of PC2 were Φ 20 and they had 115 cm (45″) legs that 80 cm (31.5″) of these legs was placed in precast beam members and the remaining length was entered into the column gap. The top main rebars of PC2 beam were 2 Φ 18 with 440 cm (173″) length that were fixed after assembling the beams and columns. In addition, 2 Φ 12 were used for temporary fixing of stirrups in the absence of the top main rebars. The bottom main rebars of beams were 3 Φ 16 with 200 cm (200″) length. All the tensile strength and the concrete compressive strength in Specimen PC2 were equal to that of Specimen PC1.
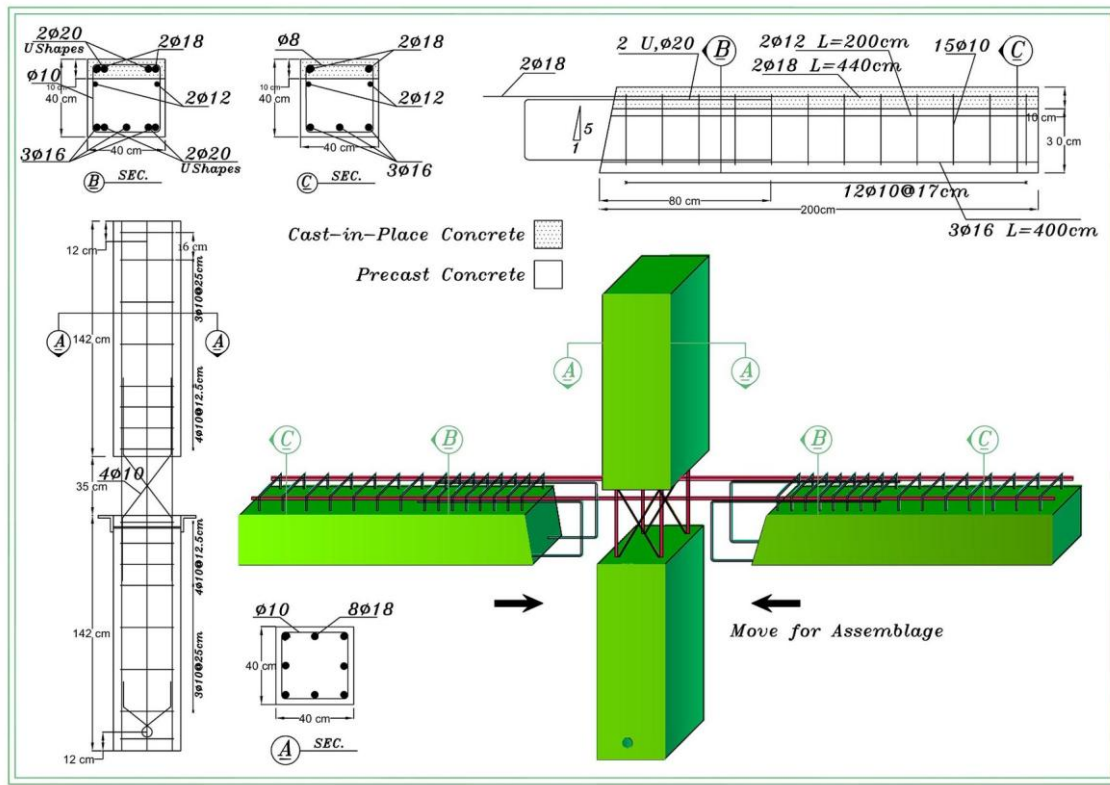
Figure 3. Dimensions and reinforcement details of Specimen PC2

U-SHAPED REBAR WITH PLATE SPECIMEN (PC3)

The detail of Specimen PC3 is shown in Fig. 4. Due to increasing the shear strength of beams connected to column in specimen PC2 and ease of fabrication in the field, a nonsymmetrical corner with longer vertical leg was provided at the joint core in the column that was projected toward beam ends. A plate with 1 cm thickness projected from beam end was seated on the smaller corner leg in each side of the column. Two U-shaped rebars were projected from column on each side and were adjusted beside the beams U-shaped rebars. In spite of PC1 and PC2 columns, there was no opening gap in PC3 column. Therefore, the connection region was only on two sides of the column, providing one separated connection area on each column face. In this specimen, continuity was cut-off in longitudinal rebars of the beams. Therefore, moments must have been transferred between beam and column only by hooked rebars and steel plates. These U-shaped bars were Φ 16 in both beams and column. Beams U-shaped bars had 115 cm (45″) legs with 35 cm (13.8″) protrusion length like beams in the specimen PC2. Columns U-shaped bars had special configuration. The top and the bottom main rebars in PC3 beam were 2Φ18 and 3Φ16 with 200 cm (79″) length, respectively. After adjustment of beams in specific situation, the plates of the beams were welded to the column steel corner and stirrups were installed and finally free spaces were filled with cast-in-place concrete. All the tensile strength and the concrete compressive

strength in PC3 were equal to those of PC1 and PC2. Since field welding was far from precast concrete constructions, it had no harmful effect on the concrete quality and it can decrease the time of beams assemblage and crane working in the field.

Figure 4. Dimensions and reinforcement details of Specimen PC3

TEST SETUP AND PROCEDURE

Fig. 5 shows the test set-up and measuring instruments. The test specimen was installed in a horizontal plane on some rollers so that it can move freely then, boundary conditions were prepared. For providing points of contra flexure in frame members subjected to lateral loads, the supports in the column bottom and top and in the end of beams were pinned and roller, respectively. Axial force was applied to the column top with a hydraulic actuator. Lateral loading was applied gradually to the column top until achieving the desired drift angle. Two linear variable displacement transducers (LVDTs) were prepared for the beam end movement in roller supports so that undesirable support movements could be controlled. Output data from these LVDTs during the test showed that the support movement was negligible. An Ultra Sonic sensor was adjusted on a fixed frame close to the column top for measuring the lateral displacement. Bottom translation of the column in pinned support was fixed to laboratory strong floor, and it can be assumed that the translation movement was zero. Lateral load applied with a 200 kN hydraulic actuator to the column top in reversed

cyclic manner. A 500 kN, *S* Shaped load cell was located between actuator and loading bonnet, where the load was transferred to specimen via load cell and bonnet. This bonnet was prepared to apply forward and backward lateral loads. Fig. 6 shows lateral loading history during the test. Load applied laterally as primary cycles in load controlled method. When yielding occurred, lateral load applied in displacement controlled method until maximum drift angle was achieved. Three cycles were performed on each stage of loading. Loading in stage1 was applied up to the fine cracks observed. Load was applied in stage2 in design load level which calculated by equivalent compressive block method. Stage3 was started after design stage up to the yield of rebars. General yielding was defined by decreasing the slope of load-displacement curve. In the next stages, load was applied at 2, 2.5 and 3% drift angle in displacement control method. Finally, the test was finished after eighteen cycles were conducted. Cracks, gap openings, and failures modes were monitored at the end of each three-successive-cycle intervals in all loading stages.
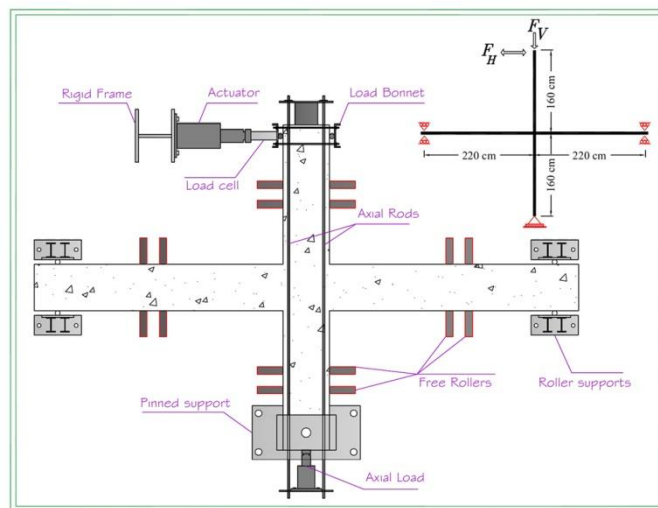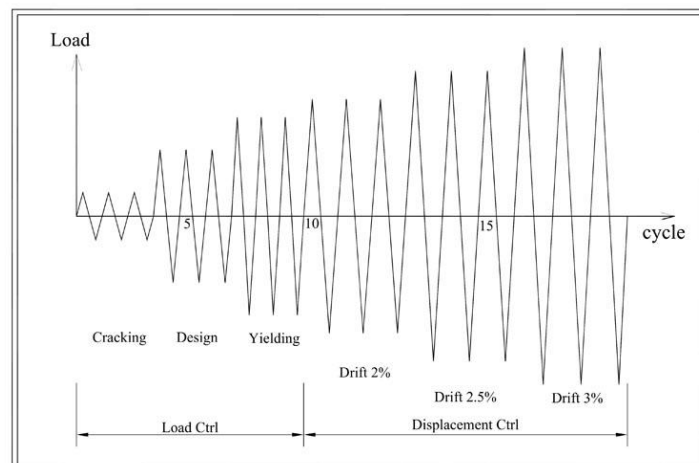

Figure 5. Test setup and instrumentations

Figure 6. Typical loading history

TEST RESULTS
MONOLITHIC SPECIMEN (MO)

Load versus drift hysteresis response of Specimen MO is presented in Fig. 7-left. Behavior of Specimen MO in the first loading stage was nearly elastic and residual displacements were less than 0.5 cm. At first, flexural cracks occurred at 38.4 kN and 0.14% drift angle. After three cycles in this step, load was increased to a design value of 51.2 kN according to Canadian concrete building code (CSA-A23.3-04) [11]. This load induced limited moment to connection for safe deformation. Then loading continued to yielding of rebars in 51.2 kN at the end of stage3. Yielding was revealed from change in load-displacement regime. Simultaneously, cracks opened from 0.4 mm to 0.8 mm adjacent to column face in bottom of the beam in the section where the rebar was yielded. In the next loading stage, load was applied to displacement control regime in 2, 2.5 and 3% drift angle. Maximum crack width at load of 110 kN was 3 mm and it increased to 5 mm at 135.8 kN load. Diagonal cracks appeared in the surface of connection core when the measured load was 130 kN in the 10th cycle. Finally, when drift angle reached to 3% - about 2 times of minimum required code value - stage2 ended and test finished. Crack took place mostly in the beam bottom due to use Φ 22 instead of Φ 28 like the beam top. Load capacity in forward and backward reversed cyclic loading was 135.8 kN and 118.5 kN, respectively. Moment capacity was about 148 kN-m which was near to ultimate value about (155 kN-m).A photo of crack pattern at 3% drift is shown in Fig. 7-Right.
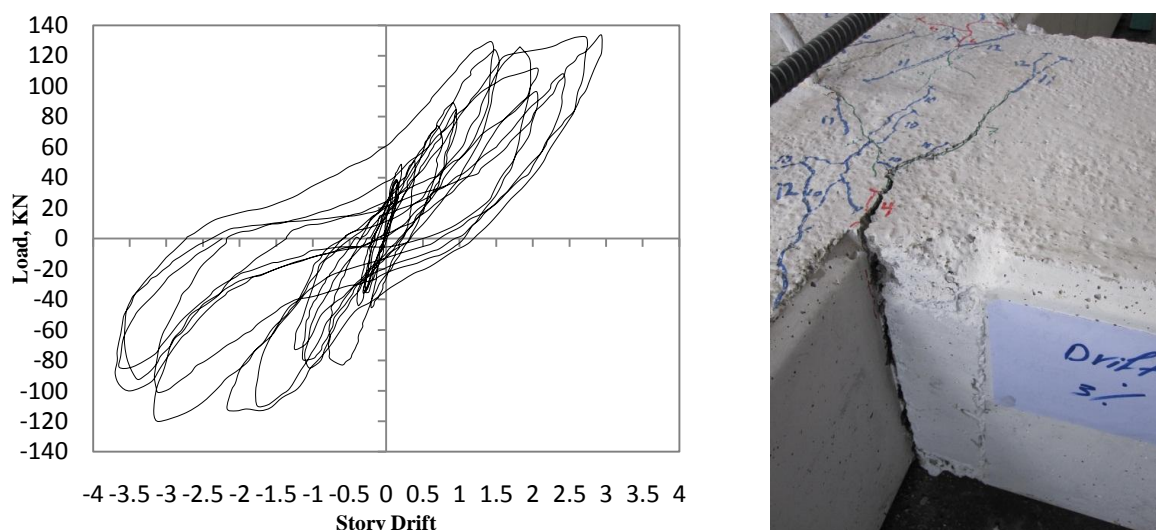

Figure 7. Lateral load versus story drift for monolithic Specimen (Left) Damage in monolithic Specimen at 3% drift angle (Right)

STRAIGHT SPLICED SPECIMEN (PC1)

Load versus drift angle hysteresis loops for Specimen PC1 is shown in Fig. 8-Left. Overall behavior of PC1 was very similar to Specimen MO in term of capacity (97% of MO) and

reinforcement percentage (ρ=1.42%), however the number of diagonal and flexural cracks were more with wider crack width. Initial obvious cracks appeared in 40 kN load. Cracks observed align the rebars on top of the beam at the second compressive load cycle. Positive and negative cracks with 0.5mm width took place in 65 kN load. Cracks spread over the middle of the beams at the 5th cycle. General yielding occurred at the 7th cycle in 0.71% drift where the applied load was 90.6 kN. Crack widths were opened more than 0.5mm and they became wider from 0.7mm to 1.25mm due to general yielding. Finally at 3% drift, load capacity of specimen decreased severely from 13.5 to 110 kN. According to Fig. 8-Right, crack concentration was in connection core while the bottom of the beam at the vicinity of column face was completely opened. Forward and backward load capacities were approximately equal to 130 kN and the moment capacity was 143 kN-m. Pinching was observed in Hysteresis loops because of extensive residual displacement and crack opening after each half cycle.
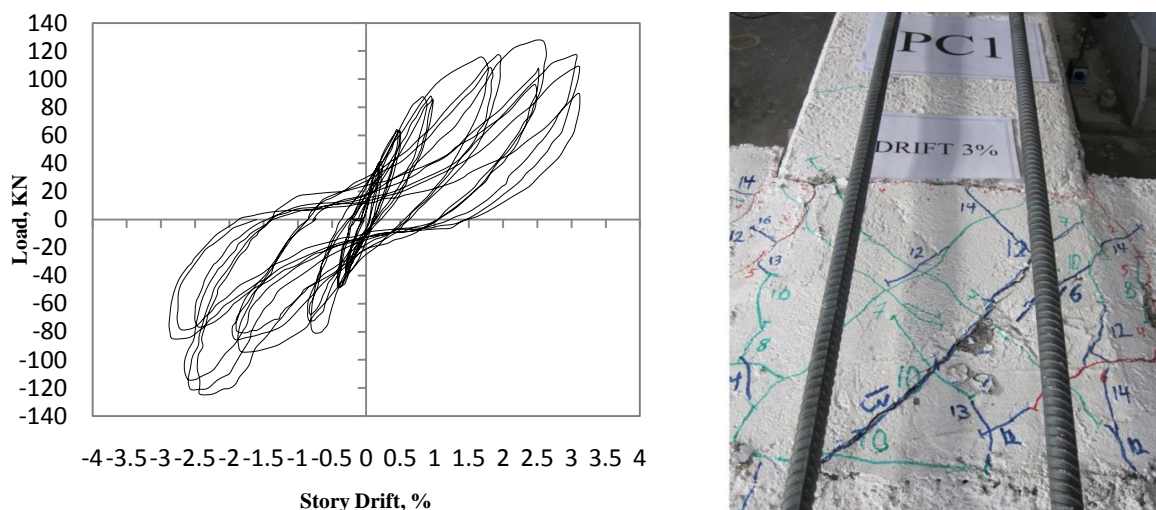

Figure 8. Lateral load versus story drift for PC1 Specimen (Left) Damage in PC1 Specimen at 3% drift angle (Right)

U-SHAPED REBAR SPECIMEN (PC2)

Hysteresis loops for Specimen PC2 are shown in Fig. 9-Left. Since rebar area in Specimen PC2 was less than Specimen MO and PC1 (ρ=1.26%), it was expectable that the moment capacity in PC2 would be less than MO and PC1 (82% of MO). Continuity of connection was provided with U-shaped rebars entered in the joint region and two straight rebars continued over the top of the beams. Three cycles were done in the first stage until initial cracks were observed in load of 49.2 kN. Then, pre-calculated design load was applied in three cycles with 7.15. Diagonal cracks were revealed in joint core; however, specimen response was still in the elastic range. General yielding was observed in 74.5 kN load. During the preceding stage, the loading changed into displacement control regime. Pinching occurred after 2% drift angle while the load was continued to 84 kN. Then load carrying

capacity was reduced to 60 kN at 2.5% drift level. In the first cycle in 3% drift angle, connection strength increased to 87.8 kN but after that, crack widening in remaining cycles at 3% drift eventually led to decrease load capacity to 65 kN. Concrete cover spalling in joint core was occurred in this drift level. A photo of crack pattern at 3% drift level is shown in Fig. 9-Right.
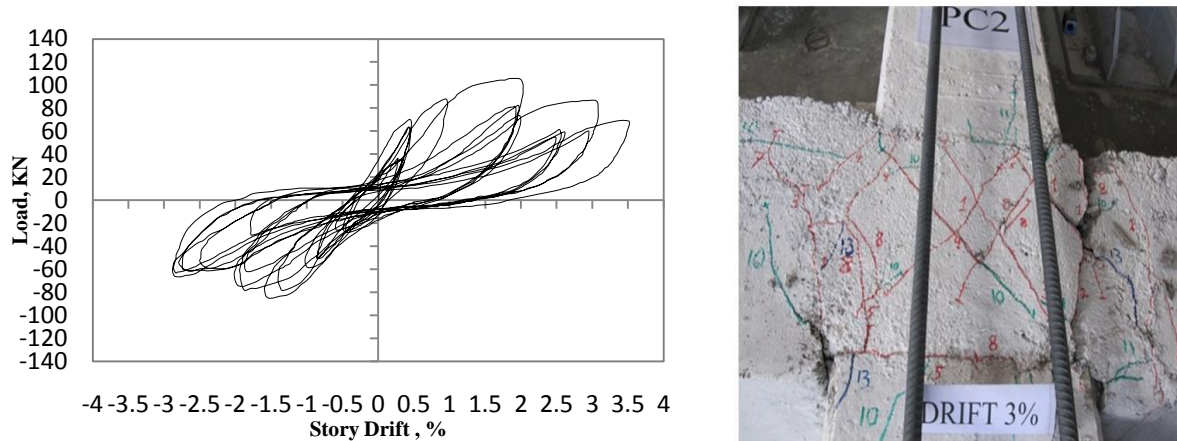

Figure 9. Lateral load versus story drift hysteresis response for Specimen PC2 (Left) Damage in Specimen PC2 at 3% drift angle (Right)

Since specimen softened at 3% drift level, load carrying capacity did not grow further than 6.5 kN. No sliding evidence was observed during the test of PC2 Specimen. It seemed that the overlapping length for the hooked bars in the connections was too short (about 35 cm). Therefore, it showed insufficient bond strength transmission mechanism. If the special stirrups used in the connection core, the shear strength will increase resulting in improvement of connection behavior. This mechanism was incorporated by inserting a steel plate in both precast beam and column in specimen PC3.

U-SHAPED REBAR WITH PLATE SPECIMEN (PC3)

The hysteresis loops of specimen PC3 are shown in Fig.10-Left. As a result of ineffective bond length adjacent to column face for specimen PC2, the idea of inserting steel plates in both column and beams was created. With respect to lower steel area in connection joints (ρ =1.34, half of plate section area was taken to account) and lower moment arm from roller supports (91% of MO), moment resistance capacity of PC3 was expected about PC2.

Specimen cracked at 35 kN in first forward loading at top of the right beam. Cracks at top and bottom of the right beam were adjoined together in the third cycle. Crack was observed in the middle of the beams in the 5th cycle. Crack widths reached 1mm at 55 kN in 6th cycle, and then increased to 1.25 mm at 1.22% drift in 7th cycle. Cracks did not extended more after 5th cycle; however they were concentrated at cast-in-place concrete region. Crack widths reached to 6 mm in 2.5% drift and enlarged to 1 cm in 17th cycle in 3% drift. In the first cycle at 3% drift, moment capacity decreased to about one-fourth and half of its

maximum value in forward and backward loading, respectively.

The most important issue in PC3 was the generation of two plastic hinges at each of the connected beams. As shown in Fig.10-Right, this behavior caused the maximum damage occurred away from the column joint core which was the most susceptible damage area in monolithic connections.

After the end of test, investigation revealed that the hooked bars were yielded and slipped which were the main severe damaging reasons.
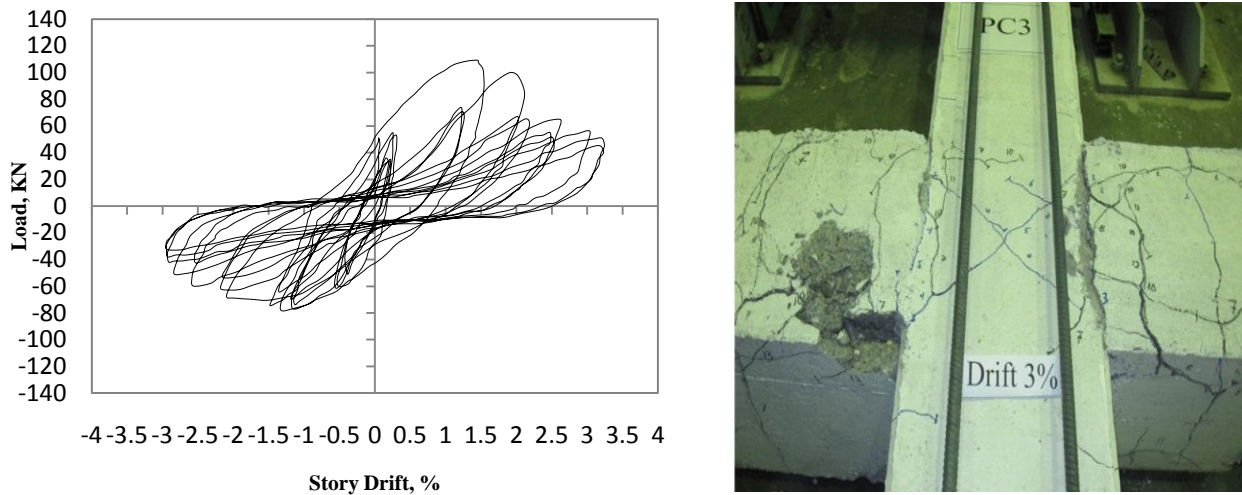

Figure 10. Lateral load versus story drift response for Specimen PC3 (Left) Damage in Specimen PC3 at 3% drift angle (Right)

EVALUATION OF TEST RESULTS

Seismic behavior of Specimens MO, PC1, PC2 and PC3 were compared together with respect to dynamic parameters such as: stiffness degradation, energy dissipation, damping ratios and ductility factors. All of these parameters are non-dimensional values to eliminate different connection details and strengths.

ENVELOPE CURVES

Fig. 11 shows the load-drift envelopes of all specimens. As expected, curves related to MO and PC1 were more similar because of similarities in the connection details and rebar ratios. Curves of specimens PC2 and PC3 have descending parts after the maximum capacity reached. The damages in these two specimens were higher than the others as shown in Figs. 9 and 10.
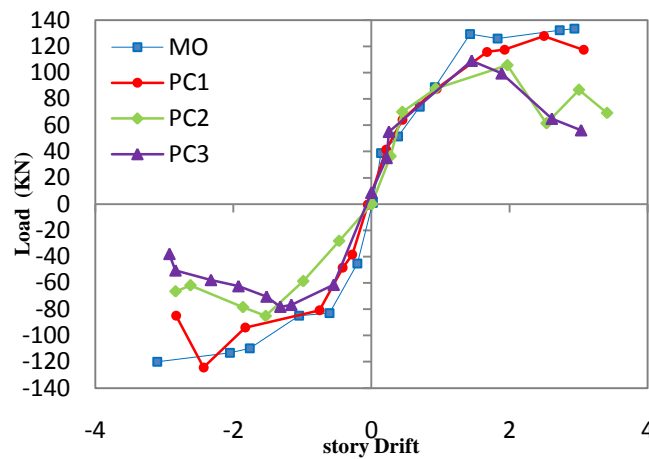
Figure 11. Envelope hysteresis curves of all specimens

STIFFNESS DEGRADATION

Stiffness of the specimens was calculated using the hysteresis load–displacement curves. Variations in the stiffness of structure members affect its behavior under the earthquake excitation. The slope of the curves can provide a relative measure for comparing the stiffness of the specimens. The secant (peak-to-peak) stiffness (K_{sec}) was calculated using a straight line drawn between the maximum load and corresponding drift points for the positive and negative directions in a loading cycle.

Variation in normalized stiffness (K_{sec}/K_{ini}) at the last cycle of each successive three cycles during the test under reversed cyclic load is shown in Fig. 12. Figure is normalized by dividing all the stiffness (K_{sec}) in each cycle by initial stiffness (K_{ini}). As a result, the use of normalized stiffness allows easy comparison with non-dimensional parameters. PC1 showed a higher normalized stiffness than the other specimens, even for the monolithic Specimen before 15th Cycle. Specimen PC3 showed a poor behavior where the stiffness was decreased severely after the first cycle.
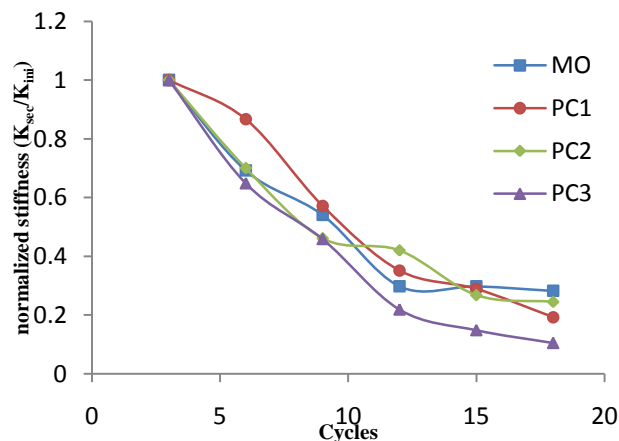

Figure 12. Stiffness degradation of specimens

ENERGY DISSIPATION

The energy dissipation capacity of a connection is calculated based on the area under the hysteresis load–deflection curve which indicates how effectively a connection withstands earthquake loadings. The typical way of comparing the energy dissipation is to plot the cumulative dissipated energy versus the number of load cycles applied. As shown in Fig. 13, energy dissipation in all precast specimens was higher than those of Specimen MO. It can be perceived from Fig. 13 that the dissipated energy in PC2 and PC3 was higher in primary cycles due to early damage. These results might be affected with differences in connection details and specimen strength because energy is not a non-dimensional parameter.
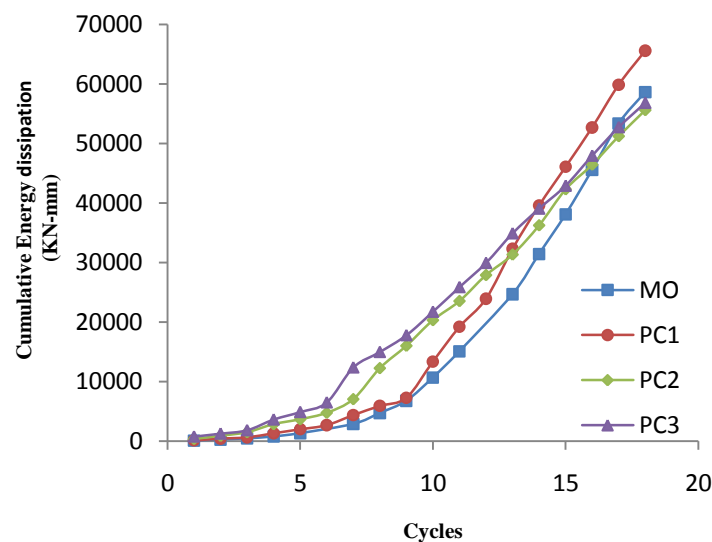

Figure 13.Cumulative dissipated energy versus ductility ratio for specimens

DAMPING RATIO

Damping ratio is a non-dimensional parameter and a well-known way to compare energy dissipation capacity in specimens. To discuss the energy dissipation characteristics of the test specimens, the equivalent viscous damping ratio ζ_{eq} was plotted against the number of cycles. The definition of viscous damping introduced by Chopra [16] is expressed by Equation 1. Hysteretic energy (A_p) and elastic peak to peak strain energy (A_e) are shown in Fig. 14. The definition of K_{sec} is also shown in Fig. 14.
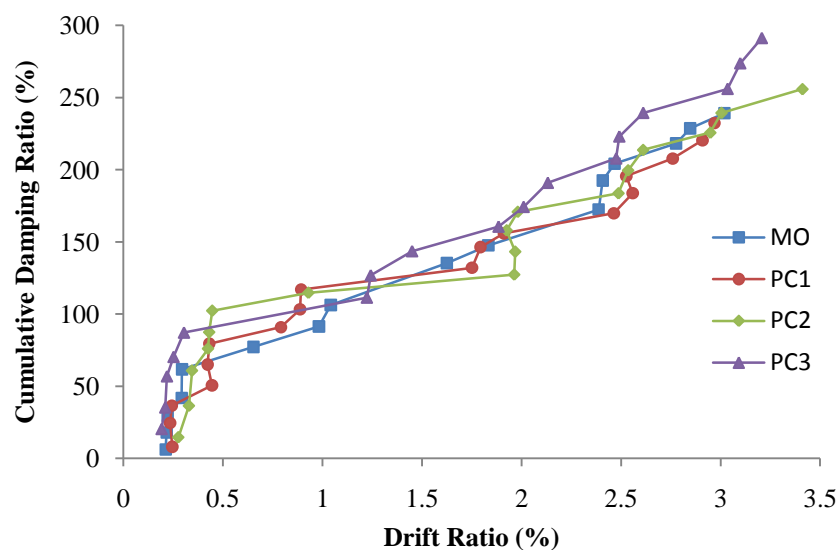
Figure 14. Schematic view of elastic peak to peak strain energy (A_e) and dissipated energy (A_p)

$$\zeta_{eq}(\%) = \frac{1}{2\pi}\frac{A_p}{A_e}\times 100 \tag{1}$$

According to Fig. 15, damping in PC3 was higher than other specimens. However, PC1, PC2 and MO had similar damping variation during the test.
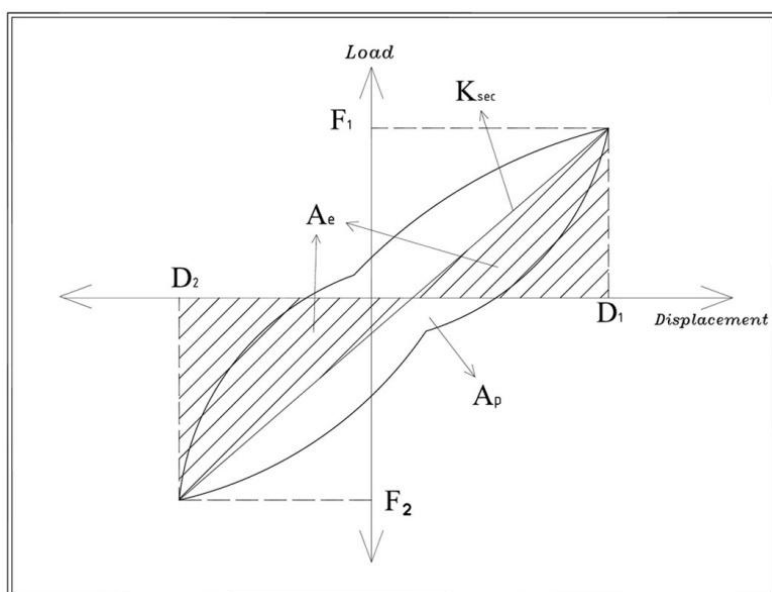

Figure 15. Equivalent damping ratio versus drift ratio for specimens

DUCTILITY RATIO

Structure ability to deform in inelastic range is further than its elastic state which it is called ductility factor. Ductility is a necessary parameter in seismic behavior to avoid brittle failure and is expressed as capacity of energy dissipation. Ductility factors in precast specimens with their ultimate load capacity relative to Specimen MO are compared in Table 4. By a definition, the ultimate load capacity was occurred after 15% decreasing of load capacity ($0.85P_{max}$). In table 1, Δ_y and Δ_u are yielding and ultimate displacement, respectively, μ is ductility factor and P_{max} and P_{MO} are the maximum load capacity in each specimen and Specimen MO.

Table 4: Ductility factor and maximum ratio of tolerated load for all specimens

	Δ_y (mm)	Δ_u (at $0.85P_{max}$)	$\mu(\Delta_u/\Delta_y)$	P_{Max}/P_{MO}
MO	38	106	2.79	1.00
PC1	35.2	99.5	2.82	0.86
PC2	37.7	64.3	1.7	0.75
PC3	30.4	64	2.1	0.73

It can be perceived that Specimen PC1 can preserve its strength and behave in a ductile manner. Ductility factor in Specimen PC2 was the smallest value among the other specimens. Specimen PC3 had the least load capacity between precast specimens while its ductility factor was greater than PC2.

The test results of three types of precast concrete beam to column connections and their monolithic counterpart subjected to reversed cyclic loads were reported. The conclusions and design recommendations are summarized as follows:

Behavior of monolithic Specimen was satisfactory in terms of strength and ductility, and the behavior of precast Specimen PC1 was very close to cast-in-place. Pinching occurred in precast specimens and it was more significant in Specimens PC2 and PC3 at higher drift levels.

Specimen MO had no strength degradation until drift 4%, whereas it was 11%, 35% and 53% for Specimens PC1, PC2 and PC3, respectively.

Stiffness degradation in PC1 was less than the others, even for Specimen MO, until 2% drift angle. Stiffness in Specimen MO was higher than PC2. Specimen PC3 had similar stiffness degradation compared with monolithic Specimen. This parameter became similar in all specimens up to 2% drift.

Monolithic Specimen had a good energy dissipation characteristic. Energy dissipation in all precast specimens was higher than that of Specimen MO due to more dissipation mechanisms.

Strength, stiffness and ductility of specimen PC2 improved by employing a steel plate in PC3 connection region to sustain shear stresses and moments in company with U-shaped rebars.

All specimens had reasonable seismic behavior even up to two times of almost all the building code requirements and they are applicable in moderate to high seismic zones.

NOTATIONS

d: Effective depth of section

Φ : Deformed bar

ρ : Rebar area ratio

K_{sec}: The secant (peak-to-peak) stiffness

K_{ini}: The Initial stiffness

ζ_{eq} : Equivalent viscous damping ratio

A_e : Elastic peak to peak strain energy

A_p : Hysteretic energy

Δ_y : yielding displacement

Δ_u : Ultimate displacement

μ : Ductility factor

P_{max} : Maximum load capacity in each specimen

P_{MO} : Maximum load capacity in Specimen MO

REFERENCES

1. Seckin M, Fu HC. Beam–column connections in precast reinforced concrete construction, *ACI Structural Journal,* **3**(1990) 252–61.
2. Soubra K, Wight JK, Naaman E. Fiber reinforced concrete joints for precast construction in seismic areas, *ACI Structural Journal,* **1**(1991) 214–21.
3. Soubra K, Wight JK, Naaman E. Cyclic response of fibrous cast-in-place connections in precast beam–column subassemblages, *ACI Structural Journal,* **3**(1993) 316–23.
4. Ertas O, Ozden S, Ozturan T. Ductile connection in precast concrete moment resisting frame, *PCI Journal,* **3**(2006) 2-12.
5. Restrepo J, Park R, Buchanan A. Tests on connections of earthquake resisting precast reinforced concrete perimeter frames of buildings, *PCI Journal,* **4**(1995) 44-61.
6. Alcocer S, Carranza R, Navarette D, Martinez R. Seismic test of beam-to-column connections in a precast concrete frame, *PCI Journal,* **3**(2002) 70-89.
7. Khoo H, Li B, Yip K. Tests on precast concrete frames with connections constructed away from column faces, *ACI Structural Journal,* 10(2006) 18-27.
8. Pampanin S. Experimental investigation on high-performance jointed ductile connections for precast frames, *Proceeding of the First European Conference on Earthquake Engineering and Seismology*, Geneva, Switzerland, 2006, pp. 2038-48.
9. Cheok G, Stone W, Stanton J, Seagren D. Beam to column connections for precast concrete moment resisting frames, *Fourth Joint Technical Coordinating Committee on Precast Seismic Structural Systems*, Tsukuba, Japan, 1994.

10. Li B, Leong W, Leong C. Hybrid-steel concrete connections under reversed cyclic loadings, *Proceeding of the Pacific Conference of Earthquake Engineering*, Christchurch, New Zealand, 2003, pp. 126-33.
11. CAN/CSA-A23.3-04. *A National Standard of Canada. Design of Concrete Structures*, Approved July 2007, Reaffirmer 2010.
12. Park H, Im H, Kang S. An experimental study on beam-column connections with precast concrete U-shaped beam shells, *Proceeding of the 14th World Conference on Earthquake Engineering,* Beijing, China, 2008.
13. Lee L, Kim S, Moon J. An experimental study of the structural behavior on the precast concrete beam-column interior joint with splice type reinforcing bars, *Journal of Architectural Institute of Korea*, **10**(2004) 53-61.
14. Khaloo A, Parastesh H. Cyclic Loading of Ductile Precast Concrete Beam-Column Connection, *ACI Structural Journal*, **3**(2003) 291-96.
15. Khaloo A, Parastesh H. Cyclic Loading Response of Simple Moment-Resisting Precast Concrete Beam-Column Connection, *ACI Structural Journal*, **4**(2003) 440-45.
16. Chopra A. *Dynamic of Structures -Theory and Applications to Earthquake Engineering*, International Edition, New Jersey, Prentice Hall, 1995.